Asociación Argentina
de Mecánica Computacional

Mecánica Computacional Vol XXVII, págs. 2195-2219 (artículo completo)
Alberto Cardona, Mario Storti, Carlos Zuppa. (Eds.)
San Luis, Argentina, 10-13 Noviembre 2008

REDUCED MODEL OF A BAR IMPACTING AN OBSTACLE USING KARHUNEN-LOÈVE BASIS

Fernando S. Buezas[a,b], Thiago G. Ritto[c] and Rubens Sampaio[c]

[a]*Dept. of Physics, Universidad Nacional del Sur, 8000 Bahía Blanca, Argentina, fbuezas@gmail.com*
[b]*CONICET, Argentina*
[c]*Dept. of Mechanical Engineering, PUC-Rio, 22453-900 Rio de Janeiro, Brasil, thiagoritto@gmail.com, rsampaio@mec.puc-rio*

Keywords: Karhunen-Loève Basis, Reduced Model, Nonlinear dynamics

Abstract. This work aims to discuss the Karhunen-Loève Decomposition and its capacity of capturing the non–linearities of a nonlinear dynamical system. A model of a bar impacting an obstacle is developed, where the impact forces come from a spring system. The system of equations of this nonlinear dynamical system is discretized by means of the Finite Element Method, and then the model is reduced by means of two different bases: Normal Modes and Karhunen-Loève Basis. The construction of the Karhunen-Loève Basis is discussed in details for both Direct Method and Snapshots Method. The numerical results show that Karhunen-Loève Basis is the most efficient basis to project the dynamics studied.

1 INTRODUCTION

Karhunen–Loève Decomposition (KLD) were developed around 1960, but its applications in solid mechanics are relatively new (Breuer and Sirovich, 1991). Even though it is each time more used in solids mechanics, KLD still lacks of basic bibliography. This works brings a simple example of a nonlinear problem that aims to elucidate the potentiality of this technique.

The vibroimpact system analyzed in this work is discretized by means of the Finite Element Method. Then a reduced order modeling is performed to compress the system of equations. This is achieved through two different bases: the Normal Modes and KL-basis. The dynamic responses are simulated, the bases are contructed and the numerical results are discussed.

There are various approaches concerning reduced order modeling. A good introduction to the subject is made by Morand. and Ohayon (1992). Spottswooda and Allemang discuss the literature of model reduction for nonlinear dynamics. In the present work it will be discussed model reduction through the Normal Modes and through KL-basis.

Karhunen–Loève basis (KL-basis) is a statistical method that aims to obtain a compact representation of a data. It has the capacity to describe the phenomenon of interest in a reduced dimension that is able to capture most of the phenomenon. KL-basis, also called Empirical Modes or Proper Orthogonal Modes (POMs), is the best basis of projection for the Galerkin method in the sense that it minimizes the average squared distance between the original data and its reduced linear representation. Nevertheless, nothing is said about how efficient this basis is in terms of time processing in a dynamical analysis.

In the beginning, KLD has appeared in the literature as Principal Components Analysis (PCA) only as a tool for signal analysis. Later it was extended for imaging processing, and then to a diverse number of applications (Holmes et al., 1996). In Mechanical Engineering its first applications were in turbulence, Lumley (1970).

KLD aims to obtain the dominant characteristics of a dynamic response obtained through experimental or numerical data. The interest of this work is the application of this technique in structural nonlinear dynamics. The group of PUC-Rio is working in this subject for a while: Sampaio and Wolter (2001), Wolter et al. (2002), Wolter (2001), Sampaio and Bellizzi. And recently Trindade et al. (2005), Bellizzi and Sampaio, Sampaio and Soize (2007).

The article is organized in the following manner: in section 2 the weak formulation of the problem is presented. In section 3 the dynamical system is discretized by means of the Finite Element Method. In section 4 the model is reduced through: Normal Modes, KL-direct, KL-snapshots. In section 5 the numerical simulations are performed, so the efficiency of the bases used in the Galerkin Method is discussed. And, finally, in section 6 the concluding remarks are pointed out.

2 PROBLEM MODELING

Consider the bar represented in Figure 1.

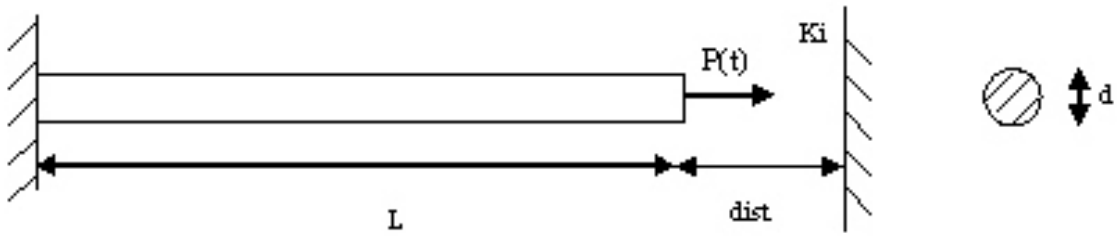

Figure 1: Scheme of a bar impacting an obstacle

The boundary conditions are given by:

$$u(0,t) = 0 \quad (dirichlet\ or\ essential) \quad EA\frac{\partial u}{\partial x}(L,t) = 0 \quad (newman\ or\ natural) \tag{1}$$

Where $x = 0$ is the fixed end and $x = L$ is the free end.

The weak formulation of the problem, considering the transversal area (A) and the material properties (E and ρ) constants in x, and adding a dissipation term (viscous damping), can be written by the following expression (Meirovitch, 1997):

$$\begin{aligned} \rho A \int_0^L \frac{\partial^2 u(x,t)}{\partial t^2}\phi(x)dx + c\int_0^L \frac{\partial u(x,t)}{\partial t}\phi(x)dx + \\ + EA\int_0^L \frac{\partial u(x,t)}{\partial x}\frac{d\phi(x)}{dx}dx = \int_0^L f(x,t)\phi(x)dx \end{aligned} \tag{2}$$

With initial conditions:

$$u(\cdot,0) = \mathbf{u}_0 \qquad \frac{du}{dt}(\cdot,0) = \dot{\mathbf{u}}_0 \tag{3}$$

Where:

$u(x,t)$ is the longitudinal displacement;
A is the transversal section area;
E is the elasticity modulus of the material;
ρ is the density of the material;
c is the damping coefficient;
$f(x,t)$ is the excitation force;
$\phi(x)$ is the trial function.

The problem is to find $u(\cdot,t) \in V$, considering equations (2) and (3), for all $\boldsymbol{\phi} \in V$, where V is the admissible space:

$$V = \mathcal{H}^1(\Omega) = \{\boldsymbol{\phi} : [0,L] \to \mathbb{R} \mid \phi(0) = 0\ and \int_0^L \left(\frac{d\boldsymbol{\phi}}{dx}\right)^2 < \infty\} \tag{4}$$

$\mathcal{H}^1(\Omega)$ is the Sobolev space and $\Omega = [0, L]$.

Because of the natural boundary condition, $\dfrac{\partial u}{\partial x}(L,t) = 0$. And because of the essential boundary condition, $\phi(0) = 0$.

The dynamic response will be approximated by $u_n(x,t) = \sum_{i=1}^{n} a_i(t)\phi_i(x)$, where a_i is the i-th generalized coordinate and $\boldsymbol{\phi}_i$ is the i-th trial function.

Substituting the approximated response into the dynamics, equation (2), considering already the boundary conditions of the problem and that the error is orthogonal:

$$\begin{aligned} &\ddot{a}_i(t)\rho A \int_0^L \phi_i(x)\phi_j(x)dx + \dot{a}_i(t)c \int_0^L \phi_i(x)\phi_j(x)dx \\ &+a_i(t)EA \int_0^L \frac{d\phi_i(x)}{dx}\frac{d\phi_j(x)}{dx}dx = \int_0^L P_L(t)\phi_j(x)dx \end{aligned} \tag{5}$$

Where:

$$\begin{aligned} &[M(\boldsymbol{\phi}_i,\boldsymbol{\phi}_j)] = \rho A \int_0^L \phi_i(x)\phi_j(x)dx \quad , \quad [K(\boldsymbol{\phi}_i,\boldsymbol{\phi}_j)] = EA \int_0^L \frac{d\phi_i(x)}{dx}\frac{d\phi_j(x)}{dx}dx \\ &[C(\boldsymbol{\phi}_i,\boldsymbol{\phi}_j)] = c \int_0^L \phi_i(x)\phi_j(x)dx \qquad\qquad F(\boldsymbol{\phi}_j) = \int_0^L P_L(t)\phi_j(x)dx \end{aligned} \tag{6}$$

The bar is excited on its free extremity and the movement of the bar is limited by an obstacle. The impact is modeled by an elastic force, proportional to the obstacle stiffness. The shocks between the bar and the obstacle introduce nonlinearity to the system. The force P_L includes the excitation force and the force due to the impacts:

$$P_L = P_f sin(\omega_f t)\delta(x - x_L) + F_c(t)\delta(x - x_L) \tag{7}$$

Where:

$$F_c(t) = -\gamma\left[k_i(u(L,t) - dist)\right] \quad \begin{cases} \gamma = 0 & if \quad u(L,t) < dist \\ \gamma = 1 & if \quad u(L,t) > dist \end{cases} \tag{8}$$

$u(L,t) \rightarrow$ displacement at $x = L$
$dist \rightarrow$ distance from the bar to the obstacle
$k_i \rightarrow$ obstacle stiffness

The discrete system becomes:

$$[M]\ddot{\mathbf{a}}(t) + [C]\dot{\mathbf{a}}(t) + [K]\mathbf{a}(t) = \mathbf{F}(t,\mathbf{a}) \tag{9}$$

Note that **F** depends on the system configuration **a**, what makes the system nonlinear. The response in the physical coordinates are recovered simply using the relationship $\mathbf{u} = [\Phi]\mathbf{a}$, where $[\Phi] = [\boldsymbol{\phi}_1\ \boldsymbol{\phi}_2\ ...\ \boldsymbol{\phi}_n]$.

3 FINITE ELEMENT METHOD

The Finite Element Method (FEM) is a discretization strategy. There is a spatial discretization and the trial functions (interpolating functions) of each element are written in local coordinates.

The element used has a linear interpolation functions. The local coordinates goes from $\xi = -1$ to $\xi = 1$, as it is showed in the Figure 2.

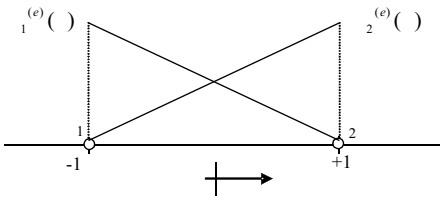

Figure 2: Linear Interpolation Functions

The elementary functions for the linear approximation are given by:

$$\varphi_1^{(e)}(\xi) = \frac{1-\xi}{2} \qquad \varphi_2^{(e)}(\xi) = \frac{1+\xi}{2} \tag{10}$$

The element matrices are:

$$[M^{(e)}] = \frac{\rho A \Delta x^{(e)}}{6} \begin{bmatrix} 2 & 1 \\ 1 & 2 \end{bmatrix} \tag{11}$$

$$[K^{(e)}] = \frac{EA}{\Delta x^{(e)}} \begin{bmatrix} 1 & -1 \\ -1 & 1 \end{bmatrix} \tag{12}$$

$$[C^{(e)}] = \frac{c}{\rho A}[M^{(e)}] \tag{13}$$

Where $\Delta x^{(e)}$ is the size of the element. The approximation used this time is $u^{(e)}(\xi, t) = \sum_{i=1}^{2} u_i^{(e)}(t)\varphi_i^{(e)}(\xi)$, where u_i is the displacement of the i-th node. The element matrices must be mapped into the global matrices $[M]$, $[K]$ and $[C]$.

The discrete system becomes:

$$[M]\ddot{\mathbf{u}}(t) + [C]\dot{\mathbf{u}}(t) + [K]\mathbf{u}(t) = \mathbf{F}(t, \mathbf{u}) \tag{14}$$

FEM is wildly used an it is very effective. Nevertheless, depending on the problem we have to deal with huge matrices. Besides that, a nonlinear analysis can be very time consuming.

4 REDUCED MODELS

The standard model considered is the one achieved by the FEM:

$$[M]\ddot{\mathbf{u}}(t) + [C]\dot{\mathbf{u}}(t) + [K]\mathbf{u}(t) = \mathbf{F}(t, \mathbf{u}) \tag{15}$$

Matrices $[M]$, $[C]$ and $[K]$ have dimensions $m \times m$. Considering $[Q]$ with dimensions $\mathbb{R}^{m \times n}$ ($n \ll m$), composed by independent vectors, we do a change in the variables:

$$\mathbf{u}(t) = [Q]\mathbf{a}(t) \tag{16}$$

The equation (15) becomes:

$$[M][Q]\ddot{\mathbf{a}}(t) + [C][Q]\dot{\mathbf{a}}(t) + [K][Q]\mathbf{a}(t) = \mathbf{F}(t, \mathbf{a}) \tag{17}$$

Matrix $[Q]$ is composed by orthogonal vectors, $\phi_i(x)$, that generate a reduced subspace into which the dynamics will be project. The linear decomposition can be written as: $u(t,x) = \sum_{i=1}^{n} a_i(t)\phi_i(x)$. Projecting the dynamics on the space generated by the new basis:

$$[Q]^T[M][Q]\ddot{\mathbf{a}}(t) + [Q]^T[C][Q]\dot{\mathbf{a}}(t) + [Q]^T[K][Q]\mathbf{a}(t) = [Q]^T\mathbf{F}(t, \mathbf{a}) \tag{18}$$

It is easy to see that $[Q]^T[M][Q]$ has dimension $n \times n$, so the problem turned out to be reduced from $m \times m$ to $n \times n$, $n \ll m$. One can expect to solve the time-integration problem much faster with the reduced model.

4.1 Normal Modes

The Normal Modes can be used as the trial functions in the Galerkin Method. If a linear system with proportional damping matrix is the one analyzed, then the basis generated by the Normal Modes are the optimum basis. When dealing with a nonlinear problem we have a problem because there is no such thing as Normal Modes.

The Normal Modes and the Natural Frequencies can be found by solving the following characteristic value problem:

$$(-\omega_i^2[M] + [K])\boldsymbol{\phi}_i = \mathbf{0} \tag{19}$$

Where ω_i is the i–th Natural Frequency and $\boldsymbol{\phi}_i$ is the i–th Normal Mode.

For a bar fixed in one end and free in the other, they can also be calculated directly by the analytical expression (Blevins, 1993):

$$\phi_i(x) = sin\left[\frac{(2i-1)\pi}{2L}x\right] \tag{20}$$

4.2 Karhunen-Loève Basis

Karhunen–Loève basis (KL-basis) can be used as the trial functions in the Galerkin Method and it is the optimum basis to represent a dynamic problem. Optimum basis in the minimum square sense, considering the norm in the Hilbert Space ($\mathcal{H}^1$). And, given a number of functions (n), no other linear decomposition will better represent the dynamics than KL-basis. KL-expansion is the most efficient in the sense that the projection of $u(x,t)$ on the subspace generated by $\phi(x)$ contains the maximal amount of energy (given an n). The terms KL-basis, Empirical Modes and POM (Proper Orthogonal Modes) will be used interchangeably in this text.

The system response is modeled as a second order stochastic process. There are two important assumptions: the process is stationary in time and ergodic, Bellizzi and Sampaio.

KL-basis depends on the displacement data, so dynamic responses must be simulated for different set of parameters, for instance, a specified range of excitation force: $100\ N < P_f < 200\ N$. In this case KL-basis is valid to represent systems which are excited by forces F from 100 to 200 N.

As showed in Sampaio and Wolter (2001) there are two methods for constructing KL-basis: the direct method and the snapshots method.

4.2.1 Direct Method

Let $\mathbf{u}(\mathbf{x},t) \in \mathbb{R}^3$ be a vectorial field with $\mathbf{x} \in \mathbb{R}^3$ and $t \in \mathbb{R}$. Decomposing $\mathbf{u}$ in two parts: one invariant in time $E[\mathbf{u}(\mathbf{x},t)]$ and another with zero mean $\mathbf{v}(\mathbf{x},t)$:

$$\mathbf{v}(\mathbf{x},t) = \underbrace{\mathbf{u}(\mathbf{x},t)}_{response} - \underbrace{E[\mathbf{u}(\mathbf{x},t)]}_{mean} \tag{21}$$

Then, $\mathbf{v}$ is an stochastic process with zero mean and, as a consequence, its correlation tensor equals to its autocorrelation tensor (Papoulis, 1991). If $\mathbf{v}$ is real, then the spatial autocorrelation function of two points is defined by the tensorial product:

$$R(\mathbf{x},\mathbf{x}') = E[\mathbf{v}(\mathbf{x},t) \otimes \mathbf{v}(\mathbf{x}',t)] \tag{22}$$

Considering the field:

$$\mathbf{u}(x_i, y_j, z_k, t) \tag{23}$$

Where i, j, k assume values from 1 to N_x, N_y, N_z respectively. For each instant of time there are N sample values, $N = 3 \times N_x \times N_y \times N_z$. The number 3 multiplying the expression is due to the three fields (x, y and z).

The sample can be put in order: $u_1(t), u_2(t), ..., u_N(t)$. The dynamical system displacement are experimentally measured or numerically calculated in N points in M instants of time.

$$[U] = [\mathbf{u}_1 \;\; \mathbf{u}_2 \;\; ... \;\; \mathbf{u}_N] = \begin{bmatrix} u_1(t_1) & u_2(t_1) & ... & u_N(t_1) \\ . & . & . & . \\ . & . & . & . \\ . & . & . & . \\ u_1(t_M) & u_2(t_M) & ... & u_N(t_M) \end{bmatrix} \tag{24}$$

Using the stationarity and ergodicity assumption, the variation of the field with respect to the mean value is:

$$[V] = [U] - \frac{1}{M} \begin{bmatrix} \sum_{i=1}^{M} u_1(t_i) & \sum_{i=1}^{M} u_2(t_i) & ... & \sum_{i=1}^{N} u_N(t_i) \\ . & . & . & . \\ . & . & . & . \\ . & . & . & . \\ \sum_{i=1}^{M} u_1(t_i) & \sum_{i=1}^{M} u_2(t_i) & ... & \sum_{i=1}^{M} u_N(t_i) \end{bmatrix} \tag{25}$$

The spatial correlation matrix is then constructed:

$$[R] = \frac{1}{M}[V]^T[V] \tag{26}$$

The matrix $[R]$ is symmetric by construction. It generates orthogonal eigenvectors, which are the Proper Orthogonal Modes, also called Empirical Modes. The Proper Values (POVs) are given by the eigenvalues of the matrix $[R]$. Note that the dimension of matrix $[R]$ depends only on the spatial discretization, it does not depend on the time discretization. Therefore the direct method is recommended when the spatial mesh is coarse and there are many instants of time.

The algorithm to implement this kind of decomposition can be summarized by the following steps:

- Discretize the displacement data $\mathbf{u}(\mathbf{x}, t)$ in M instants of time and in N points in space, $[U]$.
- Construct matrix $E[\mathbf{u}(\mathbf{x}, t)]$ calculating the mean value in time of $[U]$.
- Calculate matrix $[V]$ using $E[\mathbf{u}(\mathbf{x}, t)]$ and $[U]$.
- Construct the autocorrelation matrix $[R]$ ($N \times N$) using matrix $[V]$.
- Calculate the eigenvalues (weight or energy) and eigenvectors (POM, Empirical Modes or coherent structures) of $[V]$.

4.2.2 Snapshots Method

A snapshot is a configuration of the system at a instant of time, $\mathbf{u}^{(m)} = \mathbf{u}(\mathbf{x}, m\tau)$, where m is the number of instants.

Using the ergodicity hypothesis:

$$\mathbf{v}^{(m)} = \mathbf{u}^{(m)} - \lim_{M\to\infty} \frac{1}{M} \sum_{m=1}^{M} \mathbf{u}^{(m)} \tag{27}$$

Then, with $\mathbf{v}^{(m)}$, we calculate the autocorrelation tensor:

$$\mathbf{R}(\mathbf{x}, \mathbf{x}') = \lim_{M\to\infty} \frac{1}{M} \sum_{m=1}^{M} \mathbf{v}^{(m)}(\mathbf{x}) \otimes \mathbf{v}^{(m)}(\mathbf{x}') \tag{28}$$

In the applications the sum will be finite:

$$\mathbf{R}_M(\mathbf{x}, \mathbf{x}') = \frac{1}{M} \sum_{m=1}^{M} \mathbf{v}^{(m)}(\mathbf{x}) \otimes \mathbf{v}^{(m)}(\mathbf{x}') \tag{29}$$

M has to be sufficiently large. Diagonalizing the tensor $\mathbf{R}_M(\mathbf{x}, \mathbf{x}')$ we have the eigenfunctions:

$$\int_D \mathbf{R}_M(\mathbf{x}, \mathbf{x})' \psi_k(\mathbf{x}') d\mathbf{x}' = \lambda_k \psi_k(\mathbf{x}) \tag{30}$$

$$\int_D \frac{1}{M} \sum_{m=1}^{M} \mathbf{v}^{(m)}(\mathbf{x}) \otimes \mathbf{v}^{(m)}(\mathbf{x}') \psi_k(\mathbf{x}') d\mathbf{x}' = \lambda_k \psi_k(\mathbf{x}) \tag{31}$$

$$\frac{1}{M} \sum_{m=1}^{M} \mathbf{v}^{(m)}(\mathbf{x}) \int_D \mathbf{v}^{(m)}(\mathbf{x}') \psi_k(\mathbf{x}') d\mathbf{x}' = \lambda_k \psi_k(\mathbf{x}) \tag{32}$$

Where D is the integration domain: in our case $\mathbf{x} = x$, therefore $D = [0, L]$. Considering:

$$a_{km} = \frac{1}{M} \int_D \mathbf{v}^{(m)}(\mathbf{x}') \psi_k(\mathbf{x}') d\mathbf{x}' \tag{33}$$

One has:

$$\sum_{m=1}^{M} a_{km}\mathbf{v}^{(m)}(\mathbf{x}) = \lambda_k \psi_k(\mathbf{x}) \tag{34}$$

Making $A_{km} = a_{km}/\lambda_k$, we can calculate the eigenfunctions:

$$\psi_k(\mathbf{x}) = \sum_{m=1}^{M} A_{km}\mathbf{v}^{(m)} \tag{35}$$

Equation (35) is telling that the orthogonal basis is a linear combination of the snapshots. To calculate A_{km}, insert equation (35) into equation (31):

$$\int_D \frac{1}{M}\sum_{m=1}^{M} \mathbf{v}^{(m)}(\mathbf{x}) \otimes \mathbf{v}^{(m)}(\mathbf{x}') \sum_{n=1}^{M} A_{kn}\mathbf{v}^{(n)}(\mathbf{x}')d\mathbf{x}' = \lambda_k \sum_{m=1}^{M} A_{km}\mathbf{v}^{(m)}(\mathbf{x}) \tag{36}$$

$$\frac{1}{M}\sum_{m=1}^{M} \mathbf{v}^{(m)}(\mathbf{x}) \sum_{n=1}^{M} A_{kn} \int_D \mathbf{v}^{(m)}(\mathbf{x}')\mathbf{v}^{(n)}(\mathbf{x}')d\mathbf{x}' = \lambda_k \sum_{m=1}^{M} A_{km}\mathbf{v}^{(m)}(\mathbf{x}) \tag{37}$$

Using the internal product, $\langle\cdot\rangle$, instead of the integral:

$$\frac{1}{M}\sum_{m=1}^{M} \mathbf{v}^{(m)}(\mathbf{x}) \sum_{n=1}^{M} A_{kn}\langle \mathbf{v}^{(m)}, \mathbf{v}^{(n)}\rangle = \lambda_k \sum_{m=1}^{M} A_{km}\mathbf{v}^{(m)}(\mathbf{x}) \tag{38}$$

Considering that the set of snapshots is linear independent, the solution of the above equation is:

$$[D][A] = \lambda[A] \tag{39}$$

Where $[A]$ is a matrix in which the columns correspond to the eigenvectors of $[D]$:

$$[D]_{mn} = \frac{1}{M}\langle \mathbf{v}^{(m)}, \mathbf{v}^{(n)}\rangle \tag{40}$$

The construction of KL-basis results from this eigenvalue problem. Note that the dimensions of matrix $[D]$ depends only on the number of snapshots, it does not depend on the spatial discretization. Therefore the snapshots method is recommended when the spatial mesh is very refined and there are not many instants of time.

The algorithm to implement this kind of decomposition can be summarized by the following steps:

- Discretize the displacement data $\mathbf{u}(x,t)$ in M instants of time (snapshots) and in N points in space.
- Calculate matrix $[D]$ $(M \times M)$ using the field with zero mean $\mathbf{v}^{(m)}$
- Compute the eigenvalues and the eigenvectors, $[A]$, of matrix $[D]$
- Construct KL-basis using $[A]$ and $\mathbf{v}^{(m)}$

5 NUMERICAL RESULTS

The software used for the simulations was MATLAB. The ordinary differential equations (ODE) system is numerically integrated through the routine *ode45*, which is based on Runge–Kutta method of fourth an fifth order. $ode45$ uses an adaptive time–step to compute the time response. The maximum error allowed was 10^{-6}. A $\Delta t = 10^{-5}$ is used to visualize the result.

The computer used to run the simulation had: Pentium(R), 2 GB RAM and $3,2$ GHz. Figure 3 represents the bar considered in the simulations. Table 1 shows the values of the parameters used for the problem.

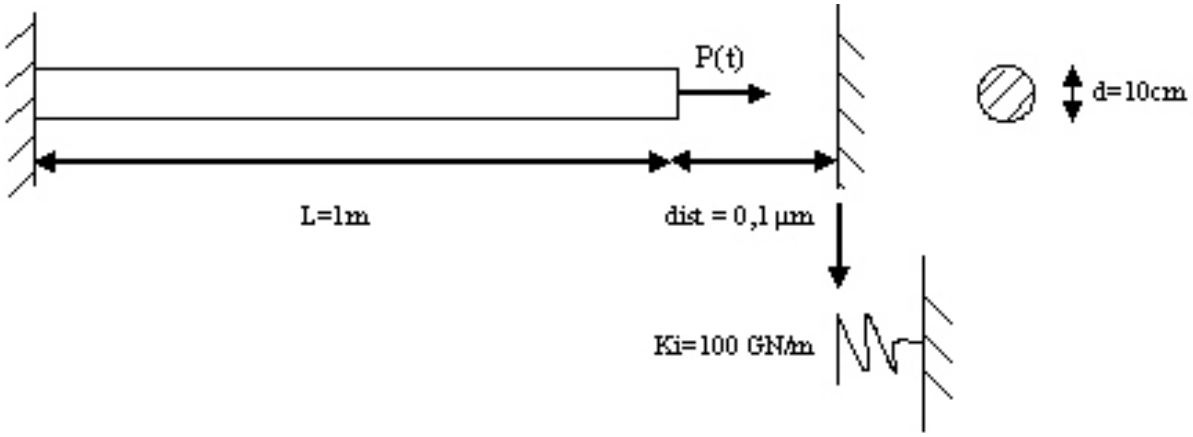

Figure 3: Bar impacting an obstacle

Length, $L = 1\ m$
Diameter, $d = 10\ cm$
Elasticity Modulus, $E = 200\ GPa$
Density, $\rho = 7850\ kg/m^3$
Damping factor, $c = 10000\ Ns/m^2$
Obstacle stiffness, $k_i = 1e11\ N/m$
Distance between bar–obstacle, $dist = 0,1\ \mu m$

Table 1: Input Data

Excitation force: $P_f sin(\omega_f t)$, $P_f = 5000\ N$ and $\omega_f = 260\ Hz$

The error analysis is made by using the following norm:

$$\|\mathbf{u}(t)\| = \sqrt{\int \mathbf{u}^2(t)dx + \int \mathbf{u}'^2(t)dx}$$

The percent error is calculated by the formula:

$$e(t) = 100 \left(\frac{\|\mathbf{u}^n(t) - \mathbf{u}^{n-1}(t)\|}{\|\mathbf{u}^n(t)\|} \right) \tag{41}$$

Where $\mathbf{u}^n(t)$ is the approximation of the response with n elements of the basis, $\mathbf{u}^{n-1}(t)$ is the approximation of the response with less than n elements and $\mathbf{u}'(t)$ is the derivative with respect to x. For the convergence analysis it will be used the average error in time $= 1/M \sum_{i=1}^{M} e(t_i)$.

5.1 Finite Element Method

The problem considered was discretized by means of the FEM. The dynamic response was calculated and the error was computed varying the number of elements:

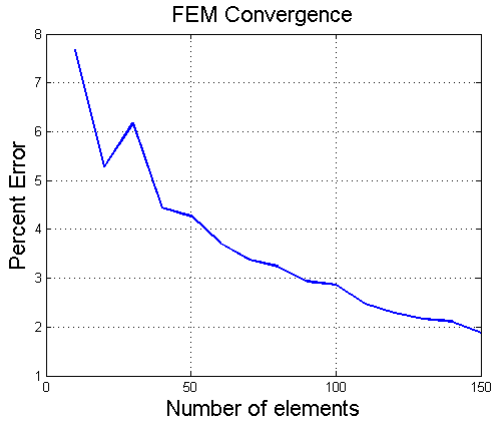

Figure 4: FEM convergence

Figure 4 shows the convergence of the approximation of the response. The precision increases with the increasing of the number of elements. For a precision of 2% it is necessary 150 elements to represent the problem.

5.2 Normal Modes

The model was reduced by means of the Normal Modes. The dynamic response was calculated and the error was computed varying the number of Normal Modes:

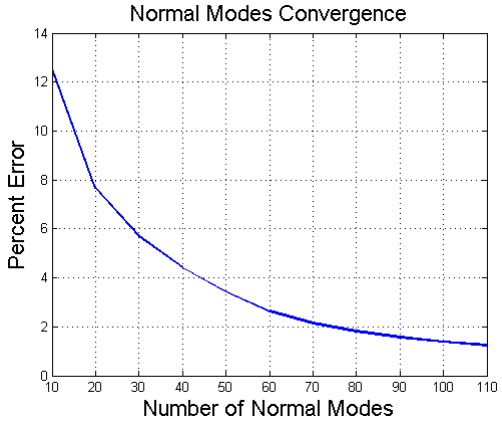

Figure 5: FEM convergence

Figure 5 shows the convergence of the approximation of the response. The precision increases with the increasing of the number of Normal Modes. For a precision of 2% it is necessary 80 Normal Modes to represent the problem.

5.3 Karhunen-Loève Basis

5.3.1 Direct Method

The model was reduced by means of the KL-basis constructed by the direct method. The dynamic response was calculated and the error was computed varying the number of Empirical Modes:

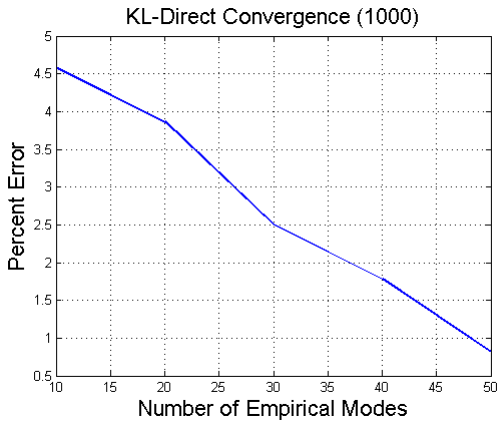

Figure 6: KL-basis convergence (using 1000 spatial points)

Figure 6 shows the convergence of the approximation of the response. The precision increases with the increasing of the number of Empirical Modes. For a precision of 2% it is necessary 40 Empirical Modes to represent the problem.

GENERATION OF KL-BASIS

KL-basis is calculated from several dynamic responses. Ten simulations $t = [0, 0.02]s$ were performed with different excitation forces, varying from 4.000 to 6.000 N. Two points should be noted:

1. KL-basis computed for a set of parameters may not be good to represent the system with another set of parameters, as it will be showed later.

2. The more data the better to get a good sample and to have a reliable KL-basis. But, to compute quickly the basis, one searches to get strictly the necessary information. In the case of KL-direct, the fewer spatial points as possible and in the case of KL-snapshots, the fewer temporal points (snapshots) as possible. This is due to how the bases are constructed.

Since only the last $0,01$ second was considered in the computations and $\Delta t = 10^{-5}$, matrix $[U]$, equation (24), has 10000 lines. To investigate the generation of the basis through KL-direct method, first we consider 1000 spatial points. The convergence analysis is shown in Figure 6.

For practical sense it is not doable to measure the displacement in 1000 points. Another KL-basis was generated considering 100 spatial points, The convergence analysis is shown in Figure 7.

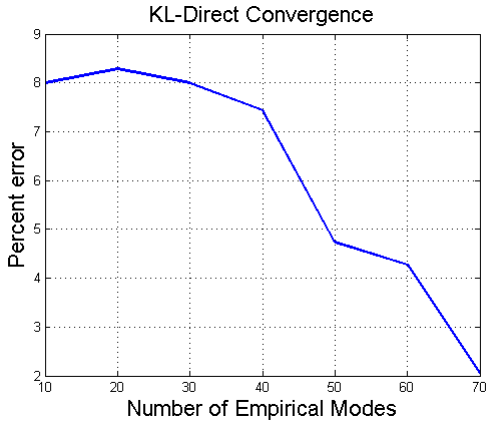

Figure 7: KL-basis convergence (using 100 spatial points)

The convergence for the KL-basis using 100 points (Figure 7) is not as good as the one using 1000. One needs 80 Empirical Modes, instead of the 40 needed before.

Considering now 10 spatial points to generate KL-basis:

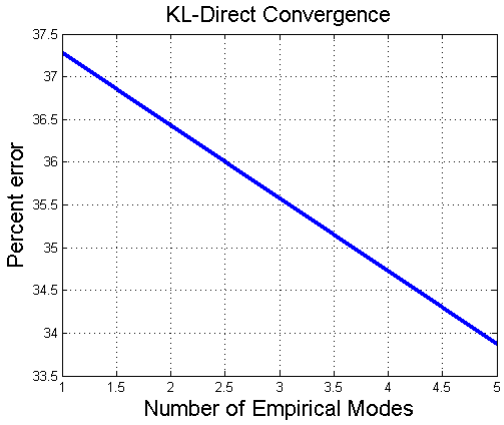

Figure 8: KL-basis convergence (using 10 spatial points)

Figure 8 shows that using only 10 spatial points the precision becomes bad. Figure 9 shows the dynamic response at $x = L$ using the KL-basis constructed with 10 spatial points. The result is not good. This means that if we use ten accelerometers for the measurements, the basis constructed with this information will not be reliable, for the problem studied.

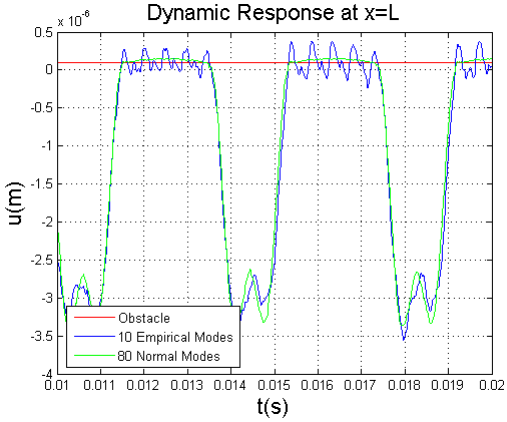

Figure 9: Dynamic response at $x = L$

Figure 10 shows a comparison between Empirical Modes and Normal Modes.

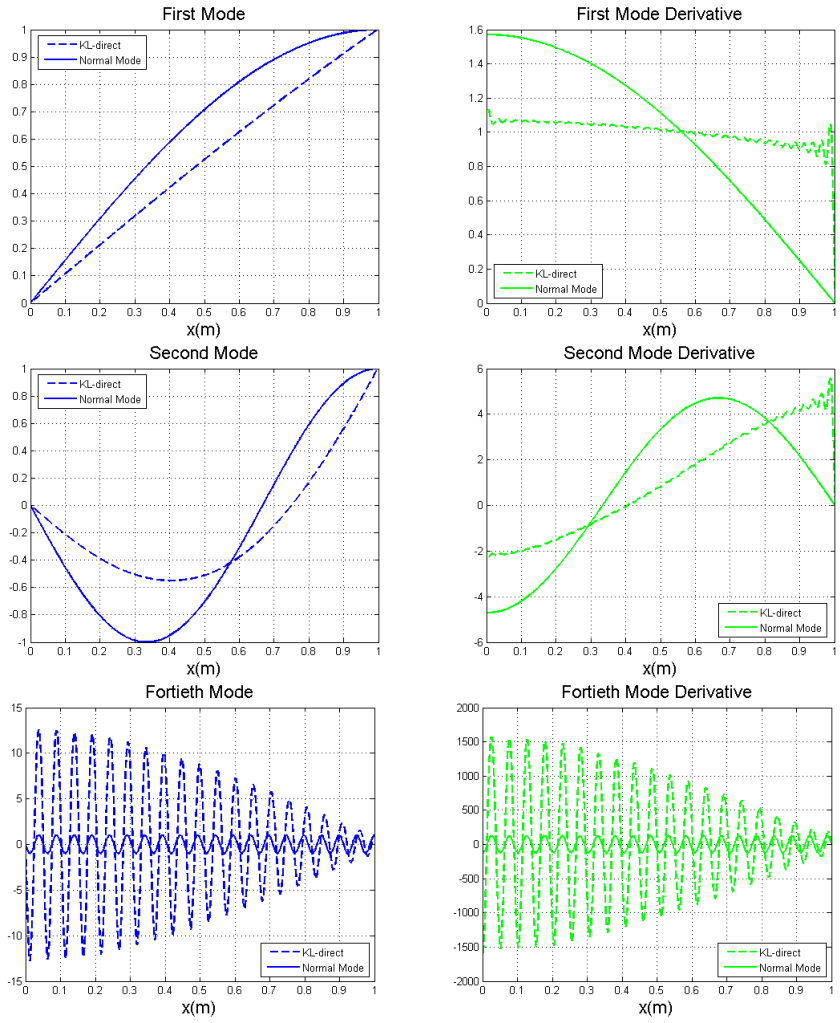

Figure 10: Normal Modes x KL-direct.

The modes have value zero at $x = 0$ and derivative equals to zero at $x = L$. The modes were

normalized to have value one at $x = L$.

The Empirical Modes are different from the Normal Modes, but their derivatives are even more different. Note that the modes derivatives are used to construct matrix $[K]$.

The shape of the Normal Modes are given by the sinus function. On the other hand, the shape of the Empirical Modes are given by the response of the nonlinear dynamics. This is the reason why they can capture the nonlinearities of the dynamics. Note that the fortieth Empirical Mode represents a shape with less amplitude close to the shock region.

5.3.2 Snapshots Method

The model was reduced by means of the KL-basis constructed by the snapshots method. The dynamic response was calculated and the error was computed varying the number Empirical Modes.

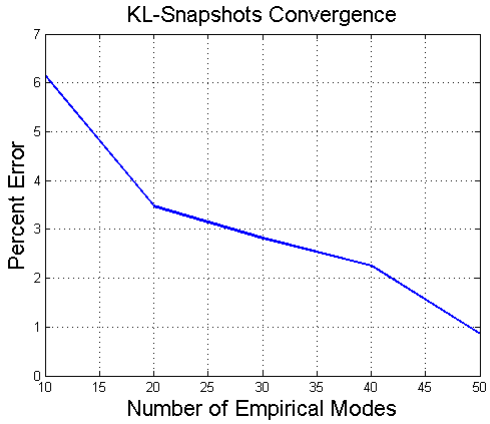

Figure 11: KL-basis convergence (using 3000 snapshots)

Figure 11 shows the convergence of the approximation of the response. The precision increases with the increasing of the number of Empirical Modes. For a precision of 2% it is necessary 50 Empirical Modes to represent the problem. It does not mean that KL-snapshots is worse than KL-direct. Comparing Figure 11 with Figure 6 we can notice that the two look very alike. For a precision of 1% it is necessary 50 Empirical Modes from both KL-direct and KL-snapshots.

GENERATION OF KL-BASIS

Three simulations were performed ($t = 0,02s$) with different excitation forces, varying from 4.800 to 5.200 N.

Matrix $[U]$, equation (24), has 3000 lines (snapshots) and 1000 columns (spatial points).

To investigate the generation of the basis through KL-snapshots method, first we consider 3000 snapshots (Figure 11). Then, we try to reduce the number of snapshots and still get a good basis. This strategy is different from KL-direct where we want to get less spatial points.

Figure 12 shows the convergence analysis for KL-basis generated with 1000 snapshots ($0,01$ second, $\Delta t = 10^{-5}$).

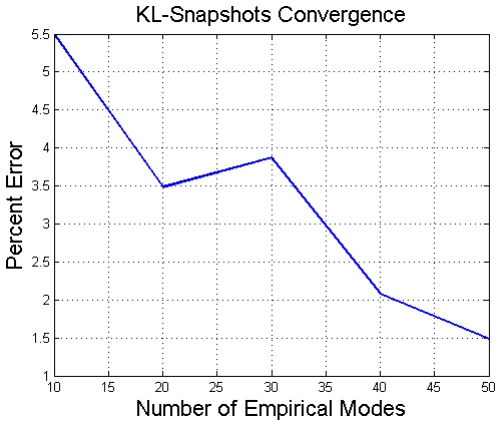

Figure 12: KL-basis convergence (1000 snapshots)

This convergence is almost as good as the one using 3000. One needs now 50 Empirical Modes for a precision of 2%.

To reduce the snapshots, but keeping the coherent structure, only one cycle of the dynamic response will be considered. Figure 13 shows the points in time where the snapshots are taken. This figure is showing only the snapshots at $x = L$, but the snapshots are taken for all of the 1000 spatial points.

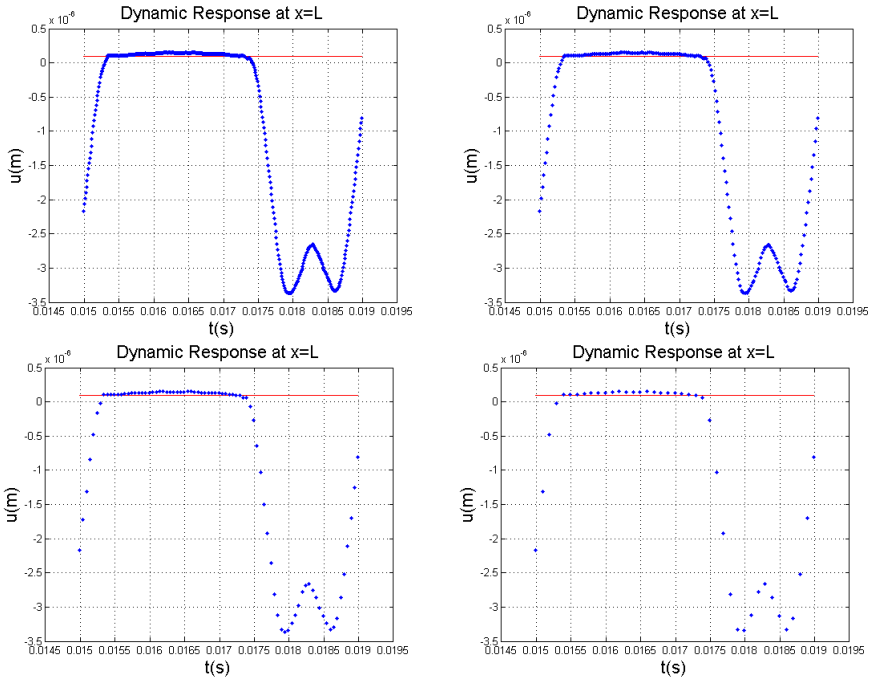

Figure 13: Temporal points where the snapshots are taken (400 snapshots, 200 snapshots, 80 snapshots and 40 snapshots)

Figure 14 shows the convergence analysis for KL-basis generated considering one cycle of the response, 400 snapshots.

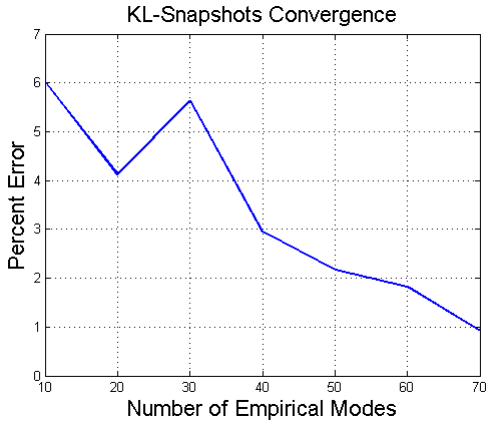

Figure 14: KL-basis convergence (400 snapshots)

This convergence is not as good as the one using 3000. One needs now 60 Empirical Modes, instead of the 50 needed before to represent the problem.

Figure 15 shows the convergence analysis for KL-basis generated considering one cycle of the response, 40 snapshots.

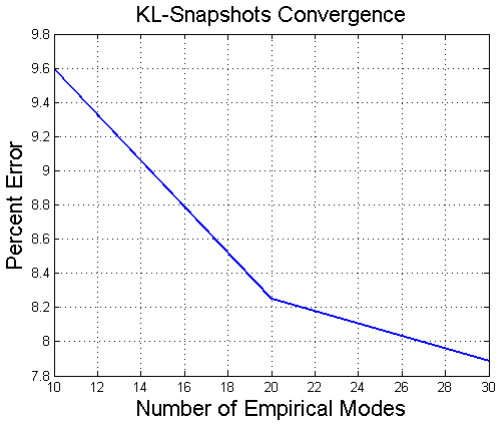

Figure 15: KL-basis convergence (40 snapshots)

Figure 15 shows that using only 40 snapshots the precision is not good. But Figure 16 shows that the response using KL-basis constructed with 40 snapshots (40 Empirical Modes) is almost as good as the one constructed with 3000 snapshots (50 Empirical Modes). The big difference is in the impact region. So, depending on the application it might be good enough.

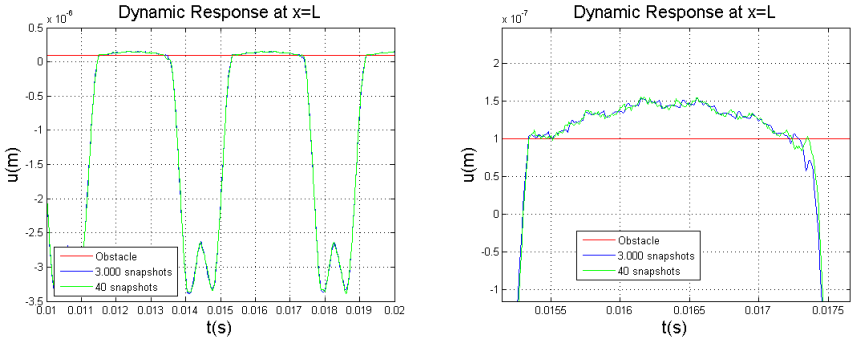

Figure 16: Dynamic response at $x = L$. Comparison between the dynamic response using two KL-basis: one constructed with 3000 snapshots (50 Empirical Modes) and another with 40 snapshots (40 Empirical Modes). At right, the impact detail.

Figure 17 shows a comparison between Empirical Modes and Normal Modes.

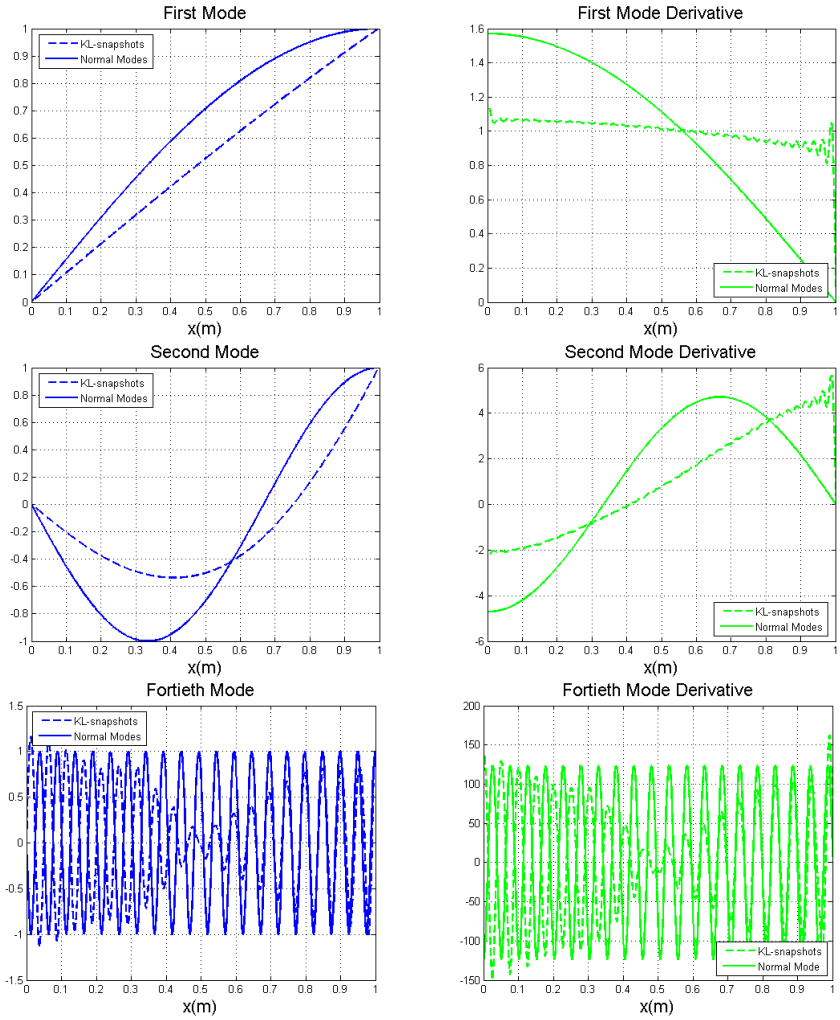

Figure 17: Normal Modes x KL-snapshots.

The modes have value zero at $x = 0$ and derivative equals to zero at $x = L$. The modes were

normalized to have value one at $x = L$. The same comments made for the Empirical Modes obtained by the direct method applied here.

The two first Empirical Modes obtained by KL-direct (Figure 10) and KL-snapshots (Figure 17) are very close to each other. They are the modes that have the most contribution to the dynamics (they are related to the highest POV). But the others Empirical Modes are different, as shows the fortieth Empirical Mode. The Empirical Modes depend on the sample used to construct the basis.

Table 2 shows the first POV (Proper Orthogonal Values) from KLD.

POV	**Direct Method**	**Snapshots Method**
λ_1	$0,998396$	$0,998498$
λ_2	$0,001472$	$0,001385$
λ_3	$0,000054$	$0,000056$
λ_4	$0,000037$	$0,000032$
λ_5	$0,000015$	$0,000014$

Table 2: POV from corresponding POM

The sum of the first five POV, for the direct method as for the snapshots method, is $> 0,9999$, what represents a high level of information of the model. This means that 99,99 % of the dynamics are in the five first POM.

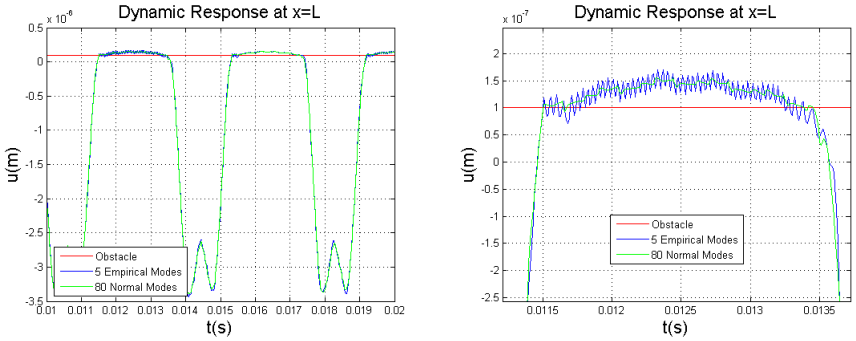

Figure 18: Approximation of the response with Five Empirical Modes. At right, the shock detail

Figure 18 shows the dynamic response at $x = L$ approximated with five Empirical Modes. One can see that the overall dynamics is well represented. But, in the shock region there is a big error. Remember that the first derivative is also computed in the error measured.

Sirovich (1987), recommends that 99% of the energy should be considered to represent the problem, but, as we see, depending on what we are interested in, 99% may not be enough.

DIFFERENT SET OF PARAMETERS

The KL-basis constructed with the set of parameter specified above was then used to approximate a problem with three different parameters: $L = 2\ m$, $c = 10\ Ns/m^2$ and $\omega_f = 800\ Hz$. Figure 19 shows two dynamic responses with a different set of parameters.

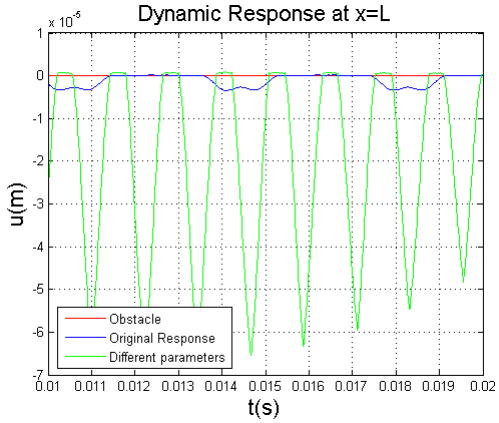

Figure 19: Dynamic Responses with two different set of parameters

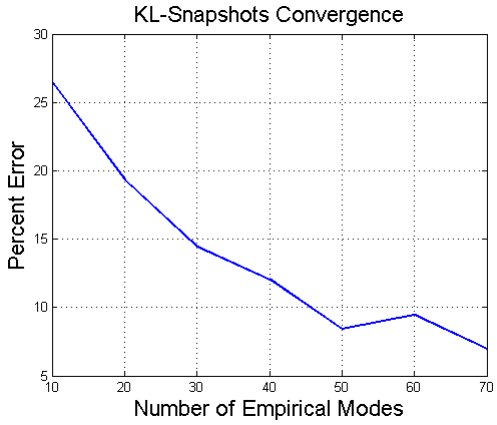

Figure 20: Convergence

Careful must be taken before using a KL-basis computed with a set of parameters for a problem with a different set of parameters. If the parameters are changed a convergence analysis must be performed to assured that the precision is maintained. In this example it is shown that the KL-basis constructed with a different set of parameters does not represent the new dynamic as well, see Figure 20 .

5.4 Dynamic Response

Figure 21 shows the dynamic response of the end point of the bar. The total simulation time was $0,02\ s$, but only the last $0,01\ s$ are considered in the analysis.

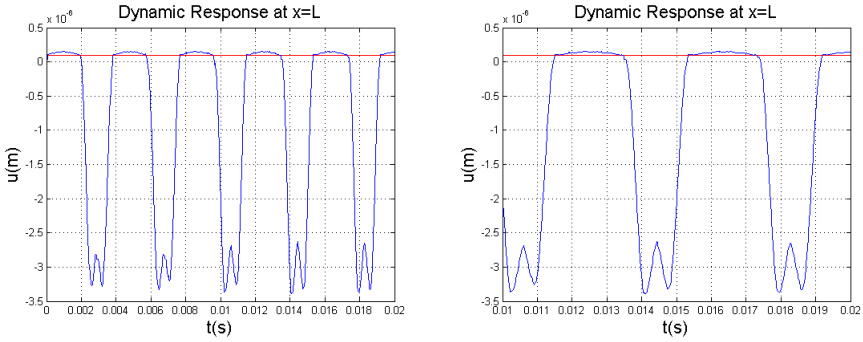

Figure 21: Dynamic response at $x = L$

Figure 22 shows a comparison between the simulations: FEM, Normal Modes, KL-basis. Using 150 finite elements, 80 Normal Modes or 40 Empirical Modes one has a good numerical response.

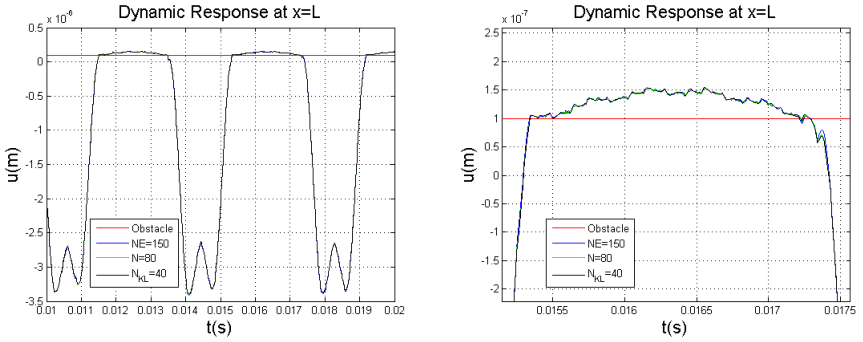

Figure 22: Dynamic response at $x = L$. FEM x Normal Modes x KL-basis. At right, impact detail.

Figure 23 shows an important point: although KL-basis is the best basis in a certain sense (given a number of elements, no other linear decomposition will represent better the problem) it is not assured that the time integration problem will be solved faster using KL-basis.

In the problem analyzed we see that: (1) specifying a precision, KL-basis will need less elements to represent the problem, but, on the other side, (2) specifying the number of elements to be used; the problem represented with the KL-basis takes more time in the numerical integration scheme, see Figure 23. An explanation for this fact is that the basis gets complicated generating matrices $[M]$, $[C]$ and $[K]$ not so well conditioned.

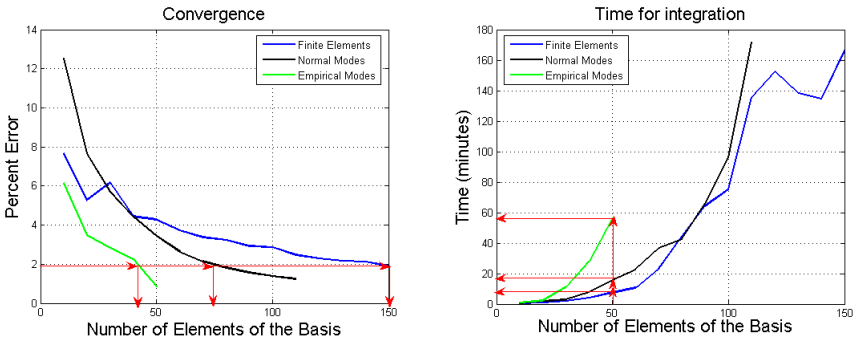

Figure 23: At left, the convergence. At right, the time spent in the numerical integration

So, we need to check the efficiency of a basis taking into account the precision wanted and the time required for the time-integration process.

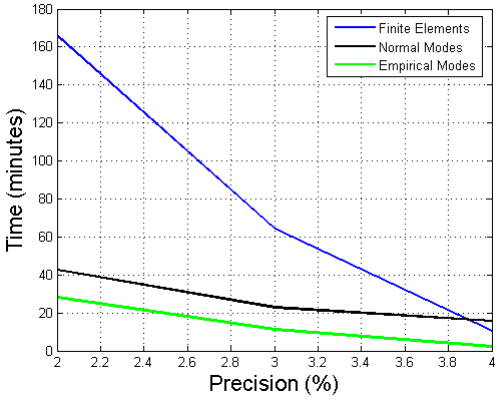

Figure 24: Precision $\times$ Time consumed at the integration process

Figure 24 shows that, for the problem in analysis, KL-basis is the most efficient one: besides making the greater reduction in the model, the time-integration process is faster, given a precision, see Table 3:

	FEM		**Normal Modes**		**KL-basis**	
Precision	NE	**Time**	N	**Time**	N_{KL}	**Time**
4%	60	11 min	50	16 min	20	2 min
3%	90	64 min	60	23 min	30	11 min
2%	150	166 min	80	43 min	40	28 min

Table 3: Precision $\times$ Time consumed at the integration process

The data used in Figure 23 for KL-basis was the one constructed through snapshots method (3000 snapshots). Figure 25 shows a comparison between KL-direct and KL-snapshots where the bases were constructed with the same amount of information (correlation matrix with dimensions 1000×1000).

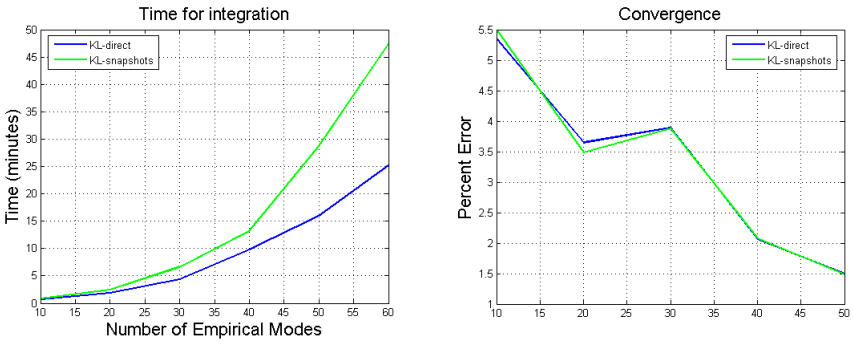

Figure 25: Simulation Time: KL-direct $\times$ KL-snapshots. At right, the convergence analysis

It is clear that both bases (KL-direct and KL-snapshots) constructed using the same sample represent the problem the same way: note how the convergence curves are almost the same. But, for the problem in analysis, the basis constructed by the snapshots method seams to be more complicated than the one constructed by the direct method because the time required for the time integration is much bigger: $28,6$ minutes (KL-snapshots) $\times$ $15,9$ minutes (KL-direct) (for 50 Empirical Modes).

6 CONCLUDING REMARKS

The potentiality of KLD was showed through a simple example of a nonlinear system. The empirical modes, obtained by KLD, generate the best projection basis to the problem.

In the example, using FEM it was necessary 150 elements to represent the problem. This high number, comparing to the approximation of the responses with Normal Modes and KL-basis, is due to the disconnection between the interpolation functions of FEM with the dynamics. Using the Normal Modes as the projection basis, 80 elements of the basis are necessary to represent the problem. Using the KL-basis, 40 elements of the basis are necessary to represent the problem. KLD is able to capture the nonlinearities of the dynamic response, therefore it can represent the problem in a reduced manner.

Besides the model reduction, other points should be highlighted:

- Even though with KL-basis we need less elements to represent a dynamics, it is not assured that the time-integration will be solved faster using KL-basis, as showed in Figure 23. But, for the problem analyzed in this paper, KL-basis is the most efficient basis, as showed in Figure 24.

- The KL-basis constructed with a set of parameters may not be good to represent a problem with a different set of parameters, as showed in Figure 20.

- Under the hypothesis of ergodicity, the sample or information needed to construct a KL-basis does not need to be so large. In the problem analyzed a correlation matrix of size 1000 x 1000 was good enough.

- 99,99% of the energy (POV) may be good enough to reconstruct the overall dynamics, but it might be bad to represent the details of a dynamic response, as showed in Figure 18.

- KL-direct or KL-snapshots? If the dynamics is complicated and the configurations complexes, it might be better to use KL-snapshots because it is constructed through the snapshots: refined mesh and few instants of time. In experimental applications it is easier to use KL-direct (few measure points), which is constructed through the dynamic response: few spatial points and many instants of time. Either way, once a basis is constructed, a convergence analysis must be performed to assure the precision needed.

- For the problem analyzed in this paper, with the same amount of information (number of spatial points equals number of snapshots) KL-direct and KL-snapshots performed the same way concerning the number of modes needed to represent the problem. Nevertheless, KL-direct performed way better concerning the time required for the time integration process, as showed in Figure 25.

ACKNOWLEDGMENTS

The authors gratefully acknowledge the support of *Conselho Nacional de Desenvolvimento Científico e Tecnológico* (CNPQ) and *Consejo Nacional de Investigaciones Científicas y Técnicas* (CONICET).

REFERENCES

S. Bellizzi and R. Sampaio. POMs analysis of randomly vibrating systems obtained from Karhunen-Loève. *Journal of Sound and Vibration*.

R. Blevins. *Formulas for Natural Frequency and Mode Shape*. Krieger Publishing Company, 1993.

K. S. Breuer and L. Sirovich. The use of the Karhunen-Loève procedure for the calculation of linear eigenfunctions. *Journal of Computational Physics*, 96(2):277–296, 1991.

P. Holmes, J. L. Lumley, and G. Berkooz. *Turbulence, coherent structures, dynamical systems and symmetry*. Cambridge University Press, 1996.

J. L. Lumley. *Stochastic tools in turbulence*. Academic Press, Inc., 1970.

L. Meirovitch. *Principles and Techniques of Vibrations*. Prentice-Hall, Inc., Upper Saddle River, New Jersey, 1997.

H. J. P. Morand. and R. Ohayon. *Interactions Fluides-Structures*. Recherches en Mathématiques Appliquées, Masson, Paris, 1992.

A. Papoulis. *Probability, Randon Variables, and Stochastic Processes*. McGraw–Hill, 1991.

R. Sampaio and S. Bellizzi. On the Karhunen-Loève basis for continuous nonlinear mechanical systems. *Anais do EUROMECH Coloquium, Nonlinear Modes and Vibrating Systems, Junho 7–9, Fréjus, França*.

R. Sampaio and C. Soize. On measures of nonlinearity effects for uncertain dynamical systems-application to a vibro-impact system. *Journal of Sound and Vibration*, 303:659–674, 2007.

R. Sampaio and C. Wolter. Bases de karhunen-loève: aplicações à mecânica dos sólidos. *APLICON 2001, EEUSP São Carlos*, 2001.

L. Sirovich. Turbulence and the dynamics of coherent structures part I: coherent strucutures. *Quarterly of Applied Mathematics*, 45, 1987.

S.M. Spottswooda and R.J. Allemang. Identification of onlinear parameters for reduced order models. *Journal of Sound and Vibration*.

M. A. Trindade, C. Wolter, and R. Sampaio. Karhunen–Loève decomposition of coupled axial/bending of beams subjected to impacts. *Journal of Sound and Vibration*, 279:1015–1036, 2005.

C. Wolter. Uma introdução à redução de modelos através da expansão de Karhunen-Loève. Master's thesis, PUC-Rio, 2001.

C. Wolter, M.A. Trindade, and R. Sampaio. Reduced-order model for impacting beam using the Karhunen-Loève expansion. *Tendências em Matemática Aplicada e Computacional*, 3: 217–226, 2002.